AN INVERSE CYCLOTRON FOR MUON COOLING*

T. Hart†, D.J. Summers, University of Mississippi-Oxford, University, MS 38677, USA

Abstract

The production of intense high energy muon beams for the next generation of particle physics experiments is an active area of interest primarily due to the muon's large mass (compared to electrons) and pointlike structure (unlike protons). The muon production and the subsequent preparation into a beam are challenging due the large emittance of the initial muon beam and the short mean muon lifetime. Most muon cooling channels being developed are single-pass structures due to the difficulty of injecting large emittance beams into a circular device. Inverse cyclotrons can potentially solve the injection problem and also reduce the muon beam emittance by a large factor. An end-to-end (injection to extraction) simulation of an inverse cyclotron for muon cooling is presented performed with G4Beamline, a GEANT-based particle tracking simulation program.

INTRODUCTION

Facilities employing intense high energy muon beams, such as neutrino factories [1], muon colliders [2, 3], and neutrinoless muon to electron conversion experiments [4] are current research and development programs for possible next generation particle physics experiments studying neutrinos, the Higgs particle, possible supersymmetric particles, and lepton number violating decays. Muon beams are produced from the decays of pions which, in turn, are produced from collisions of high-energy protons and a high-density target. A tertiary muon beam has a large emittance which must be reduced for a useful beam for experiments. Also, the short lifetime of the muon ($\sim 2.2\ \mu$s) makes the rapid ionization cooling technique necessary as opposed to standard cooling techniques for stable electrons or anti-protons.

Most muon cooling channels are single-pass structures requiring strong radio-frequency gradients and strong transverse focusing to achieve rapid cooling. Multi-pass sychrotron ring-like structures would be much less expensive than linear designs, but injecting large emittance initial muon beams is a limiting difficulty [5]. An inverse cyclotron, a cyclotron in which particles are injected at large radius and lose energy by passing through a moderator material and thus spiral in toward the cyclotron center, is such a multi-pass device with potentially large beam admittance [6].

* Work supported by National Science Foundation Award 757938 and DOE grant DE-FG05-91ER40622

† tlh@fnal.gov

THE INVERSE CYCLOTRON

The inverse cyclotron slows a muon beam to a mean kinetic energy ($K.E.$) and radius of 300 keV and 3300 mm and then to roughly 90 keV and 2200 mm. An inverse cyclotron can accept a large range of initial energies which can be slowed to the common final energy at extraction: higher energy particles will make more turns in the helium moderator and take longer time to spiral in toward the extraction region. While the energy spread of the muons is reduced from injection to extraction, the differing number of turns of muons with different initial energies increases the time spread of the beam. The beam is then extracted and guided out along the positive z direction, slowed by a uniform electric field by about 55 keV and then sent through a section of time-varying electric fields which slow the beam more while increasing the time spread. The final $K.E.$ is about 30 keV which approaches the low energies necessary for frictional cooling for possible further longitudinal phase space reduction. Frictional cooling could reduce the muon beam energy spread down to about 2 keV.

The emphasis for this inverse cyclotron configuration is on manipulation of the final low energy region in a uniform low helium density. Also, the initial beam is not injected in a single turn here, and decay processes are turned off. Some steps for further development are extending the magnetic field outward for larger initial beam energies and varying the moderator density with respect to radius for single-turn injection and more rapid energy loss.

Simulations of this muon inverse cyclotron are done by G4Beamline [7].

The inverse cyclotron consists of three sections:

- A strong focusing cyclotron field containing 0.0001 mg/cm^3 helium which slows down muons injected from outside the cyclotron. The cyclotron field is generated from curved, sectored spirals which provide radial focusing by the increase of $< B_z >$ with radius, and axial focusing through large flutter and coil spiral angle. The muon beam spirals in toward the center of the cyclotron.
- An extraction section which extracts a slowed beam from the inner portion of the cyclotron. Current coils guide the beam out along a path parallel to the z axis.
- A section to manipulate the $(t, K.E.)$ phase space. A short section is an opposing constant electric field to reduce the kinetic energies of each muon. The final section is a series of electric traps which further reduces the kinetic energy of the beam. The section of constant electric field and the series of traps are inside a long solenoid.

ISBN 978-3-95450-128-1

Strong Focusing Cyclotron Field

The cyclotron field is designed to focus strongly both radially and axially for the entire beam orbit in which the muons spiral inward while losing energy in the helium moderator. The 16-sector magnetic field is generated by 32 current carrying coils shown in Fig. 1. Each coil has total current 0.0213 MA and consists of eight line segments. The line segments are arranged so that the coil has a 30 degree spiral from 1.6 m $< r <$ 4.0 m. The z positions of the endpoints as a function of the radial locations of the endpoints are 0.6 m^2/r so that the coils get closer together as r increases to generate a magnetic field with increasing $< B_z >$ with radius.

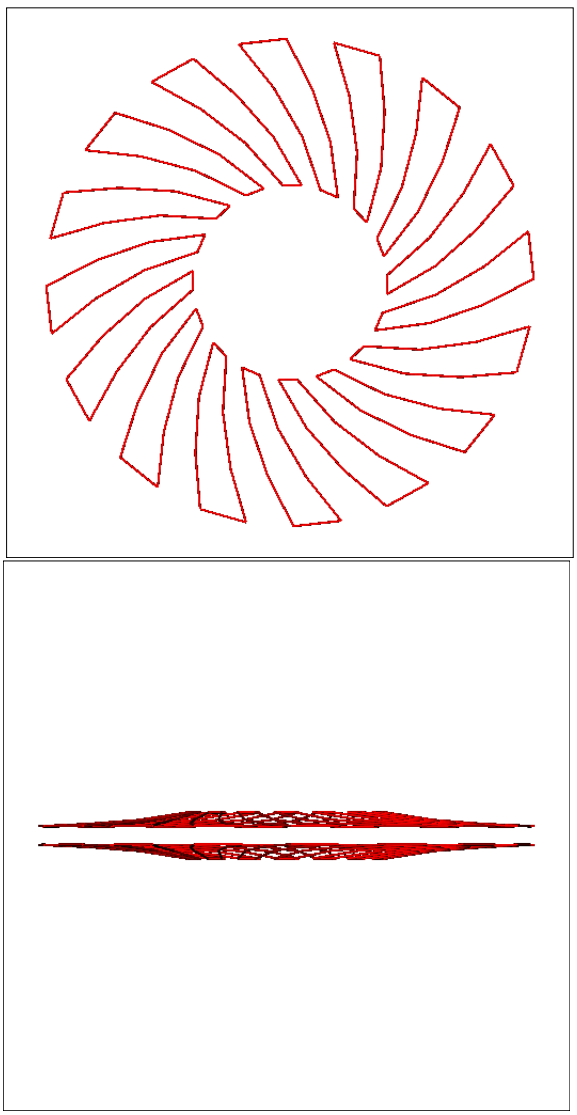

Figure 1: $x-y$ and $x-z$ views of the current-carrying coils providing the focusing magnetic field. The radial extent of the coils is 1.6 m $< r <$ 4 m, and the distance between the coils is 0.75 m at r = 1.6 m and 0.3 m at r = 4.0 m.

Figure 2 shows $B_z(r, \theta, z = 0)$, the midplane magnetic field clearly indicating the large flutter, spiral structure, and rise of $< B_z >$ with radius for 1.6 m $< r <$ 4 m.

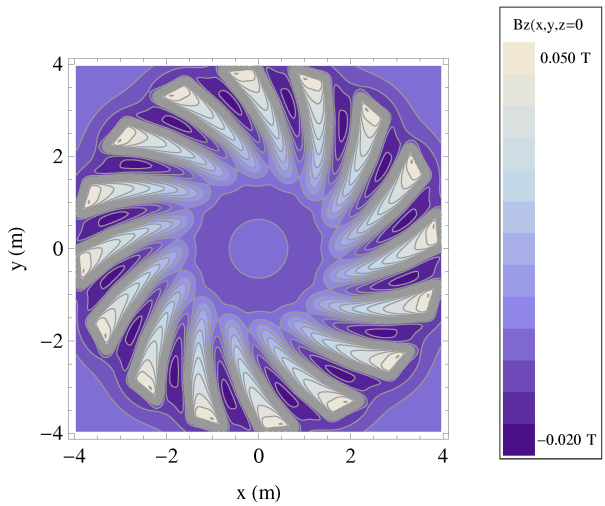

Figure 2: $B_z(z = 0)$ of the focusing magnetic field.

Figure 3 shows the tune diagram for the cyclotron field. If the phase advance of betatron oscillation per cell is kept below 90 degrees, the reduction of the dynamic aperture caused by sextupole and octupole fields can be mitigated [8]. The G4Beamline tracking simulation using 16 sectors instead of fewer sectors verifies that the phase advance is below 90 degrees and that the dynamic aperture is maintained.

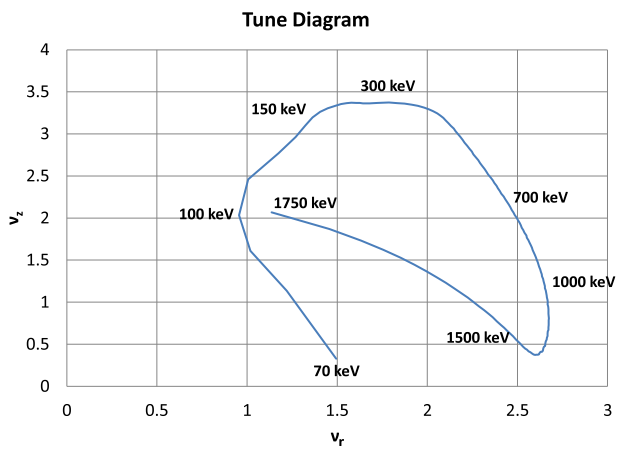

Figure 3: ν_z $vs.$ ν_r of the focusing magnetic field determined with CYCLOPS [9] closed orbit code.

Extraction Channel

After the muon beam is slowed from 300 keV down to around 90 keV spiraling in to $r \sim 2200$ mm, the beam is extracted from the region of the focusing field along two sections of equal curvature, $\rho = 1369$ mm, the first in the $x - y$ plane and the second in the $y - z$ so that the final beam direction is parallel to the z axis. The extraction field is provided by a series of current-carrying coils whose centers and axes follow the two arcs of the extraction path.

ISBN 978-3-95450-128-1

Figure 4 shows the extraction channel placed inside the focusing coils.

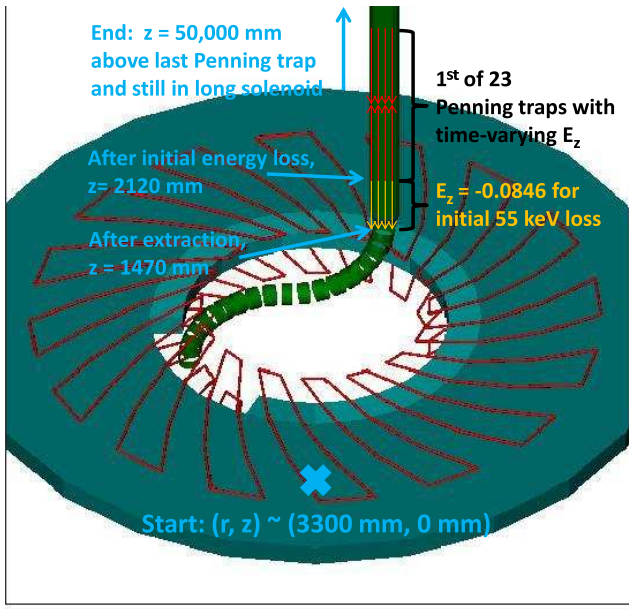

Figure 4: Arrangement of the focusing coils (red), extraction coils (green) and helium (aqua). The 650 mm long region of constant E_z and the first Penning trap are also indicated: these are surrounded by a 50,000 mm long solenoid. The locations denoted in light blue are the four places where the values and spreads of the throughgoing beam are evaluated.

The radii, length, and radial thickness of the extraction coils are 150 mm, 150 mm, and 5 mm respectively. The coils each carry 50 A/mm^2 current density and have 10 degree separation. The magnitude of the magnetic field along the coil axes is 0.1 T and reverses direction from coil to coil. The current direction alternates from coil to coil to keep the average radial field close to zero which minimizes the drift of the beam with respect to the ideal extraction path.

Longitudinal Phase Space Manipulation

Immediately after extraction, the muon beam enters a long solenoid containing a short section of opposing electric field followed by a series of electric traps with time-varying electric fields to further slow down the muon beam. The radius, length, and radial thickness of the solenoid are 200 mm, 50,000 mm, and 5 mm respectively. Each coil carries 15.625 A/mm^2 current density. The magnetic field along the long solenoid axis is 0.1 T

The muon beam passes along $+z$ through a 650 mm long section of an opposing electric field E_z of 0.0846 MV/m so that the beam $K.E.$ is reduced by 55 keV.

After this uniform energy reduction, the muon beam passes through a series of Penning traps with time-varying electric fields which reduce the beam $K.E.$ mean value while increasing the time spread.

Each trap consists of two subsections, each 1 m long along z placed next to each other along z. The lower section has an electric field E_z pointing along $+z$, and the upper section has an electric field equal in magnitude, but pointing along $-z$ so that the electric fields point toward a common midplane of constant z. The electric fields rise linearly in time from 0 MV/m to 0.005 MV/m in 300 ns after which the electric fields are held constant. The 300 ns rise time was set to accomodate the anticipated extraction beam's time spread, but the time spread turned out to be larger than expected. The maximum electric field is set so that a muon in each trap while the trap's electric field magnitude is rising will have its $K.E.$ rise and fall a few keV with an overall net energy reduction. A muon entering a trap will either be trapped if the energy is low enough and the entrance time is within an appropriate time window, or the muon will pass through exiting with a smaller $K.E.$ than the entrance $K.E.$, or will pass through exiting with a kinetic energy equal to its initial kinetic energy. Each trap's time when the electric field ramp-up is started is set so that a 50 keV muon starting at the central time in the extracted beam time spread is trapped in the last trap with $|K.E.| < 5$ keV. As the beam has time and energy spreads, very few muons will be similarly trapped, but the energies of some muons will be reduced while other muons will pass through with no net energy loss. With these trap sizes and timings, the energy spread of the beam increases slightly. This needs to be optimized.

RESULTS AND DISCUSSION

The inverse cyclotron simulation starts with an initial beam with average kinematic mean values and spreads given in Table 1. These spreads were determined with simulated beams with much larger initial spreads: the subset of the initial beam that made it through the slowing in helium, extraction along $+z$, and through the electric traps was traced back to the injection, and the initial spreads of the subset determined appropriate initial values and spreads for a beam most likely to be successfully slowed and extracted.

Table 1: Average Values and Spreads of Input Beam

r	(3289 ± 50) mm
p_r	(0.00 ± 0.32) MeV/c
z	(0 ± 15) mm
p_z	(0.00 ± 0.16) MeV/c
t	(1 ± 98) ns
$K.E.$	(305 ± 75) keV

Table 2 shows the how much of the initial beam reaches the beginning of the extraction region, the end of extraction, the end of the 650 mm region where the energy is reduced by the constant opposing electric field, and after the series of electric traps which reduce the kinetic energy further. These locations are shown in Fig. 4. Evaluations at these four locations of the inverse cyclotron are made with

ISBN 978-3-95450-128-1

the common events, about 1.6% of the full initial beam, that traverse the full path of the inverse cyclotron. Currently, only about 4% of an ideally started beam with no initial spatial, angular, or energy spreads will traverse the entire inverse cyclotron system due to losses in the helium moderator, extraction system, and longitudinal modulation system.

Table 2: Fraction of Initial Beam Remaining at various Places of Inverse Cyclotron

Location	Fraction remaining
Start ($r \sim 3300$ mm, $z \sim 0$) mm	1.000
Beginning of extraction	0.310
After extraction (z = 1470 mm)	0.024
After 55 keV reduction (z = 2120 mm)	0.017
After Penning traps (z = 50,000 mm)	0.016

The main beam losses occur between injection and the start of extraction and in the arcs comprising the extraction channel. Muons undergo stochastic scattering and energy straggling which knock even ideally started muons out of the magnetic focusing channel. The beam entering the extraction channel has large position and angular spreads so that transportation along the extraction channel will have losses. A minor beam loss also occurs from the electric field of -0.0846 MV/m which turns around a small portion of the muons.

Figure 5 shows views of an orbit that reaches the start of the extraction channel in a little over 6 turns and is subsequently extracted.

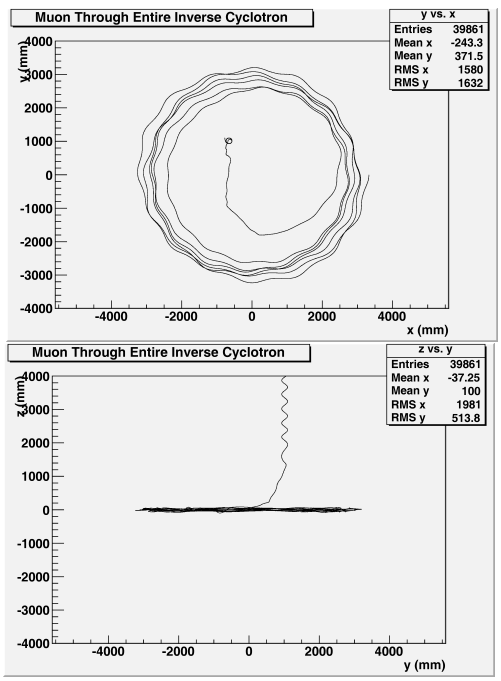

Figure 5: $x-y$ and $y-z$ views of a slowed and extracted muon. Note that the few hundred mm radial loss on the last turn is large enough to enter a 150 mm radius extraction channel.

Table 3 shows the kinematic values and spreads of the throughput beam at the four specified locations of the inverse cyclotron. Figure 6 shows the kinetic energies from Table 3, in particular, the almost 5-fold decrease in energy spread from injection to the end of extraction.

Table 3: Kinematic Spreads at Four Specified Locations of the Inverse Cyclotron of the Throughput Beam

Beam at start	End of extraction $z = 1470$ mm
$r = (3289 \pm 43)$ mm $p_r = (0.02 \pm 0.33)$ MeV/c	$x = (-638 \pm 49)$ mm $p_x = (-0.50 \pm 1.02)$ MeV/c
$z = (-1 \pm 12)$ mm $p_z = (0.03 \pm 0.15)$ MeV/c	$y = (986 \pm 42)$ mm $p_y = (-0.56 \pm 0.74)$ MeV/c
$t = (-1 \pm 102)$ ns $K.E. = (315 \pm 63)$ keV	$t = (7200 \pm 2277)$ ns $K.E = (91.6 \pm 13.8)$ keV
After initial energy reduction $z = 2120$ mm	After traps $z = 50,000$ mm
$x = (-639 \pm 63)$ mm $p_x = (-0.28 \pm 0.79)$ MeV/c	$x = (-651 \pm 63)$ mm $p_x = (-0.09 \pm 1.03)$ MeV/c
$y = (997 \pm 38)$ mm $p_y = (-0.42 \pm 1.08)$ MeV/c	$y = (1003 \pm 47)$ mm $p_y = (-0.07 \pm 0.99)$ MeV/c
$t = (7273 \pm 2281)$ ns $K.E. = (36.6 \pm 13.8)$ keV	$t = (15,530 \pm 4421)$ ns $K.E. = (33.6 \pm 14.8)$ keV

The increase in time spread from injection to the end of extraction is due to the variation of the number of turns needed to slow different energy muons to 90 keV. Muons with the lowest initial energies of about 200 keV require only 3 turns and about 3800 ns to reach the extraction while the highest energy muon to go through the entire inverse cyclotron, one with initial $K.E.$ = 546 keV, took 18 turns and almost 17,000 ns to slow down to 90 keV and go through the extraction channel.

These results indicate that this inverse cyclotron reduces the energy and energy spread of a muon beam through ionization energy loss with helium. While losing energy in helium and spiraling inward, a sectored, spiraled magnetic field with positive field index generated from current-carrying, bent, spiraled current coils provided adequate radial and axial focusing to tranport part of the muon beam to an inner extraction channel.

More work to address challenges remain for the inverse cyclotron. The time spread of the muons increases by a factor larger than the factor of energy spread reduction. The beam losses along the extraction channel can be reduced with an improved design from the initial implementation of arcs of coils with current directions alternating from coil to coil. After extraction out along $+z$, the longitudinal phase space manipulation consisting of the static electric field and time-varying electric fields of the Penning traps reduces the beam energy slightly while slightly increasing energy spread. The Penning trap sizes and timings can be

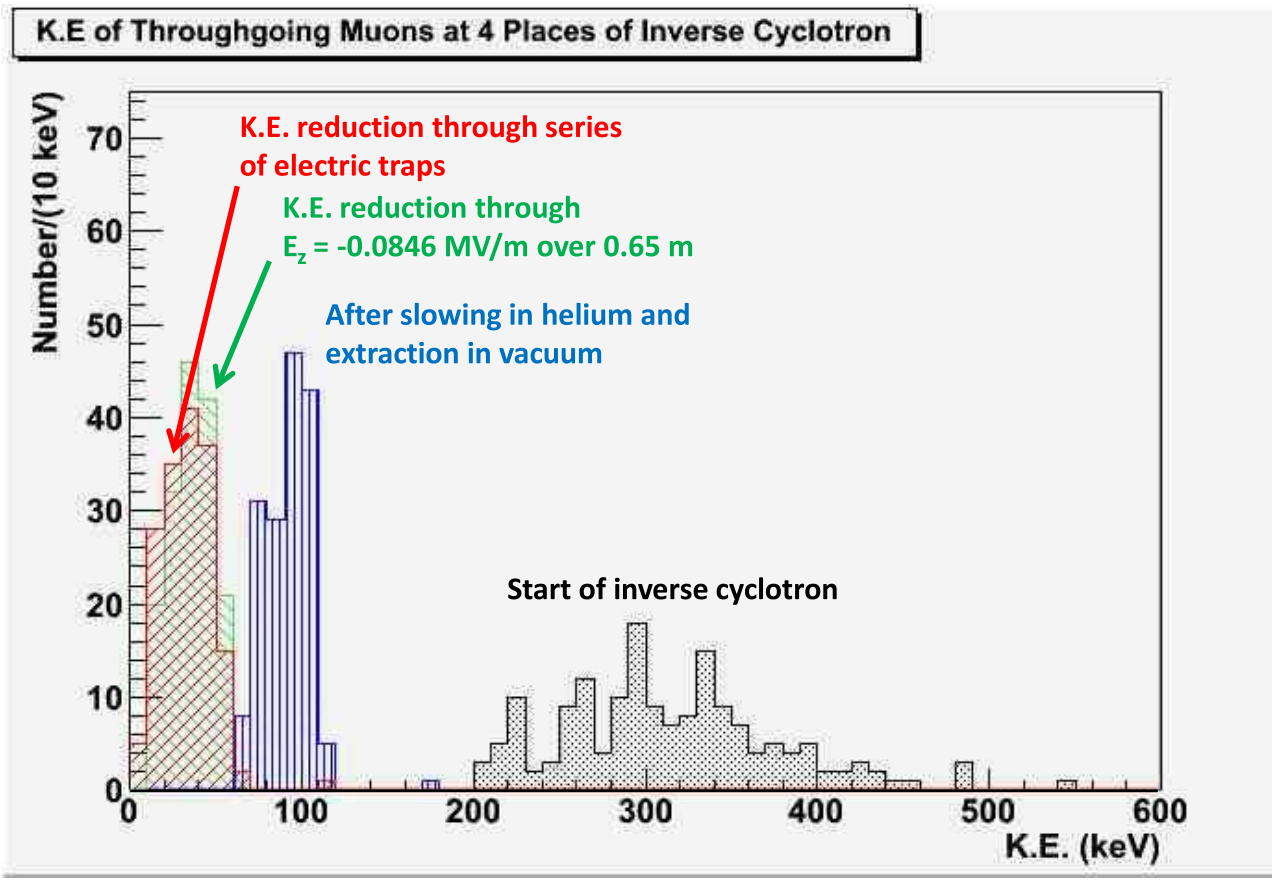

Figure 6: Kinetic energy development (right to left) from injection, after extraction, after 55 keV energy loss, and at final exit of the portion of the initial beam that went through full inverse cyclotron system.

improved and optimized to further reduce the beam energy and energy spreads if the time spread can be reduced. Also, variation of the moderator density is needed for single-turn injection, increasing the initial beam energy, and faster energy loss.

REFERENCES

[1] D. Koshkarev, CERN-ISR-DI-74-62;
M. Alsharo'a *et al.,* Phys. Rev. ST AB **6** (2003) 081001.

[2] D. Neuffer, AIP Conf. Proc. **156** (1987) 201;
R. Fernow and J. Gallardo, Phys. Rev. **E52** (1995) 1039;
J. Gallardo *et al.,* Snowmass 1996, BNL-52503;
C. Ankenbrandt *et al.,* Phys. Rev. ST AB **2** (1999) 081001;
R. Palmer *et al.,* Phys. Rev. ST AB **12** (2009) 031002;
G. Lyons *et al.,* arXiv:1112.1105

[3] R. Palmer *et al.,* arXiv:0711.4275.

[4] R. Kutschke, arXiv:1112.0242.

[5] R. Palmer *et al.,* Phys. Rev. ST AB **8** (2005) 061003.

[6] D. Summers *et al.,* Int. J. Mod. Phys. **A20** (2005) 3851;
K. Paul *et al.,* PAC-2011-MOP051;
T. Hart *et al.,* PAC-2011-WEP190.

[7] T.J. Roberts *et al.,* EPAC-2008-WEPP120.

[8] International Committee for Future Accelerators Beam Dynamics Newsletter, No. 43, p. 30, August, 2007.

[9] M.M. Gordon, Part. Accel. **16** (1984) 39.

ISBN 978-3-95450-128-1